Vehicle Feature Extraction by Patch-Based Sampling

William W. L. Lam*, Clement C. C. Pang, Nelson H. C. Yung
Department of Electrical & Electronic Engineering
The University of Hong Kong, Hong Kong SAR

ABSTRACT

In modern traffic surveillance, computer vision methods are often employed to detect vehicles of interest because of the rich information content contained in an image. In this paper, we propose an efficient method for extracting the boundary of vehicles free from their moving cast shadows and reflective regions. The extraction method is based on the hypothesis that regions of similar texture are less discriminative, disregarding intensity differences between the vehicle body and the cast shadow or reflection on the vehicle. In this novel algorithm, a united likelihood map that based on the relationship of texture, luminance and chrominance of each pixel is initially constructed. Subsequently, a foreground mask is constructed by applying morphological operations. Vehicles can be successfully extracted and different vehicle components can be efficiently distinguished by the related autocorrelation index within the vehicle mask.
Keywords: visual traffic surveillance, vehicle extraction, object segmentation, shadow detection, texture analysis

1. INTRODUCTION

With the rapid development of computer and communication technologies, the research and development of Intelligent Transportation Systems (ITS) techniques are becoming more and more ambitious and substantial [19]. Among the many facets of ITS, visual traffic surveillance plays an important role in traffic data capturing, incident detection and safety management in general. It is able to convey a comprehensive content of information that is easy for human interpretation. Such information can also be interpreted by machines if appropriate algorithms are available. Being able to interpret visual information by machines not just improves operation efficiency, but also the overall 'intelligence' of the ITS. For this reason, much research effort has been directed to finding methods that can automatically interpret the content of an image or image sequence. In order to do that, features of vehicles in an image must first be extracted for computing mean speed, flow rate, incidents, among other traffic parameters. As such, vehicle extraction has always been one of the major components of visual traffic surveillance recently [5, 6].

Segmentation algorithms that extract the vehicle of interest from the image background in an image sequence have recently been actively pursued [9, 17]. In many of these algorithms, the detection of vehicles is mainly based on their speed, dimension, luminance, chrominance and edge features from an image or image sequence [3, 4, 10, 13]. Unfortunately, these approaches suffer a major drawback that when they are applied to outdoor scenes, undesired object features, such as tree branches, cast shadows on the road, are extracted together with the vehicles. This also creates a series of problems associated with occlusion if the cast shadows are not detected and eliminated. In order to accurately detect the vehicle, numerous shadow detection methods have been proposed [1, 2, 7, 12, 15, 16]. They all suffer from a number of limitations such as specific weather conditions are required that make them ineffective in practical outdoor environments or some of them are limited to indoor environments only.

Texture analysis is an alternative way to extract vehicles effectively. A proof of the role of textural information in outdoor object recognition was done by comparison of classification correctness [8]. If textural information was used to classify an outdoor object, 99% of accuracy was achieved. Conversely, spectral information-based classification achieved only 74% of accuracy. Therefore, we propose an efficient algorithm that based on texture analysis for extracting vehicles in this paper. We assume that the textural features of moving objects are significantly different from the background. However, the studies of texture analysis of road condition and vehicles are limited [18], for that reason, a problem analysis of using texture analysis technique is briefly described in the next section. Following that, the proposed methodology is introduced in section 3. Simulation results and discussion are given in section 4. Finally, the conclusion is drawn in section 5.

*wllam@eee.hku.hk; phone 852 2857-8414

Image and Video Communications and Processing 2003, Bhaskaran Vasudev, T. Russell Hsing, Andrew G. Tescher, Touradj Ebrahimi, Editors, Proceedings of SPIE–IS&T Electronic Imaging, SPIE Vol. 5022 (2003) © 2003 SPIE–IS&T · 0277-786X/03/$15.00

2. PROBLEM ANALYSIS

Conventionally, vehicles are extracted based on their appearance and/or motion from an image or image sequence. A common first step in most recently proposed algorithms relies on subtracting a background reference image from its input image [3, 4, 9, 10, 17]. Subsequently, unwanted objects such as the cast shadow have to be removed by post-processing techniques. In order to accurately extract vehicles from an image, we aim to eliminate the cast shadow first.

Broadly, cast shadow can be defined as the darkened region on the background of an image that is due to the foreground objects blocking the light source. The luminance values of the cast shadow pixels are normally lower than those of the corresponding pixels in the background image and the chrominance values of the cast shadow pixels on the other hand, are identical or only slightly different from those of the corresponding pixels in the background image. Besides, we observed that textural feature of cast shadow is only slightly different from those of the corresponding pixels in the background image. In other words, the textual property of the background is substantially altered by the cast shadow of a foreground object. To understand this better, let us consider this textual property in depth.

Generally, texture spatial organization is often described by the correlation coefficients that evaluate linear spatial relationships between primitives. In an autocorrelation model, a single pixel is considered a texture primitive, where primitive tone property is the gray-level. If the texture primitives are relatively large, the autocorrelation function value decreases slowly with increasing distance, while it decreases rapidly if texture consists of small primitives. If primitives are placed periodically in an image, the autocorrelation function is also periodic. Texture description of an image patch is commonly calculated using the following autocorrelation function R,

$$R(u,v)=\frac{(2M+1)(2M+1)}{(2M+1-u)(2N+1-v)}\frac{\sum_{m=0}^{2M-u}\sum_{n=0}^{2N-v}p(m,n)\,p(m+u,n+v)}{\sum_{m=0}^{2M}\sum_{n=0}^{2N}p^2(m,n)}\qquad \begin{matrix}0\le u\le 2M\\ 0\le v\le 2N,\end{matrix}\tag{1}$$

where u, v is the position difference in the m, n direction, and $2M + 1$, $2N + 1$ are the dimensions of the image patch p. Based on the assumption that the image patch is periodic in the spatial domain, the autocorrelation function R can be determined in the frequency domain from the image power spectrum,

$$R=\mathcal{F}^{-1}\left\{|F|^2\right\},\tag{2}$$

where $\mathcal{F}$ is the Fourier transform. Alternatively, the autocorrelation function R can be rewritten in the spatial domain using the following equation,

$$R(u,v)=\frac{\sum_{m=0}^{2M}\sum_{n=0}^{2N}p(m,n)\,p\big((2M+1)\bmod(m+u),(2N+1)\bmod(n+v)\big)}{\sum_{m=0}^{2M}\sum_{n=0}^{2N}p^2(m,n)}\qquad \begin{matrix}0\le u\le 2M\\ 0\le v\le 2N.\end{matrix}\tag{3}$$

Essentially, the textural relationship between image frames can be evaluated by the autocorrelation function R as shown in Figure 1. Figure 1 depicts three image frames f_1, f_2, f_3, taken by a static camera and the autocorrelation results for image patches A and B of size $M = N = 16$ denoting the same locations of three image frames f_1, f_2, f_3. The profiles of the autocorrelation function R of frame f_1 and frame f_2 for image patch A are very similar as there is no moving object. Moreover, the profiles of the autocorrelation function R of frame f_1 and frame f_2 for image patch B are also very similar even the cast shadow of a bus is projected on the road of frame f_2. In frame f_3, a dark colored vehicle is at the center of the image and both image patches A and B now cover part of the vehicle. The profiles of the autocorrelation function R for image patch A and image patch B of frame f_3 are drastically different from those of frame f_1 and frame f_2 even the luminance values are lower in image patch A of frame f_3 than image patch B of frame f_2.

The autocorrelation difference d_R between two image patches can be calculated by the square difference of two autocorrelation functions R to compare their similarities,

$$d_R(u,v)=\left[R_i(u,v)-R_j(u,v)\right]^2,\tag{4}$$

where R_i, R_j are the autocorrelation functions R of two different image patches. The profiles of the autocorrelation differences d_R of image patch A and image patch B between those frames f_1, f_2, f_3 are plotted in Figure 2.

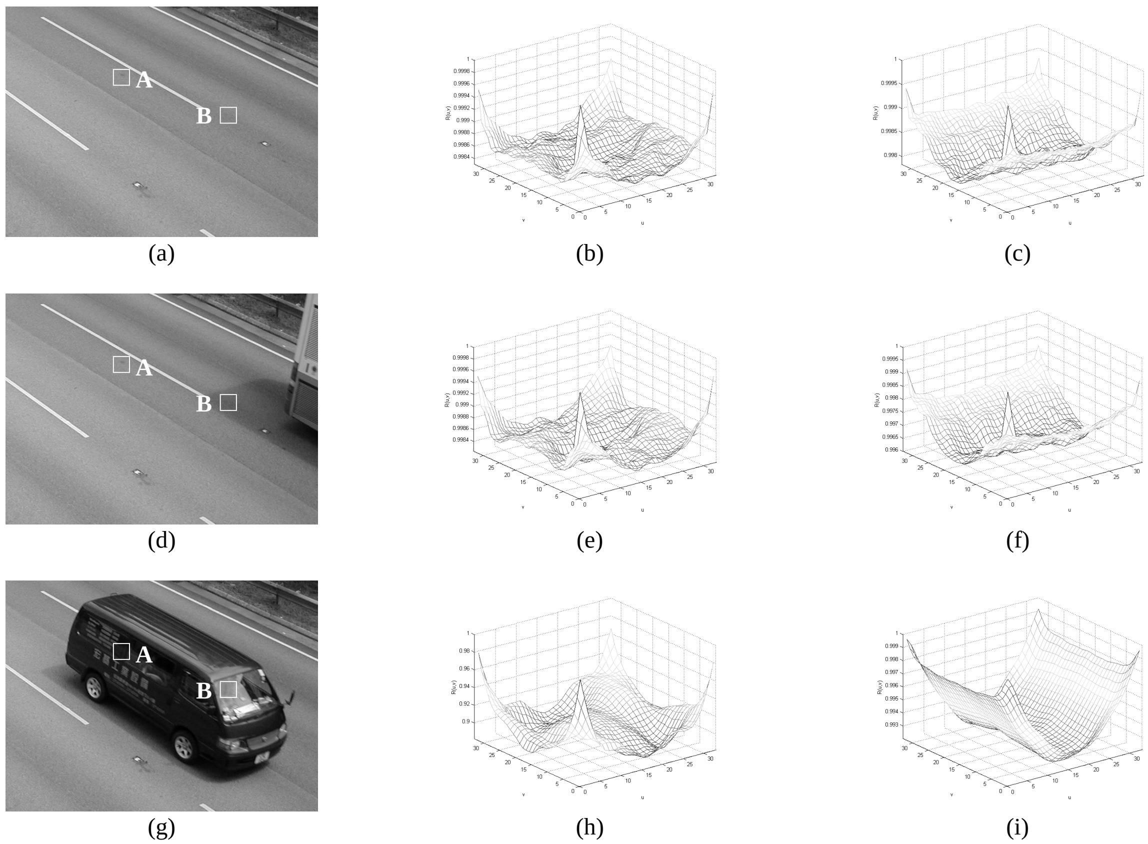

Figure 1: (a) Image frame f_1; Autocorrelation function R of frame f_1 for: (b) image patch A and (c) image patch B. (d) Image frame f_2; Autocorrelation function R of frame f_2 for: (e) image patch A and (f) image patch B. (g) Image frame f_3; Autocorrelation function R of frame f_3 for: (h) image patch A and (i) image patch B.

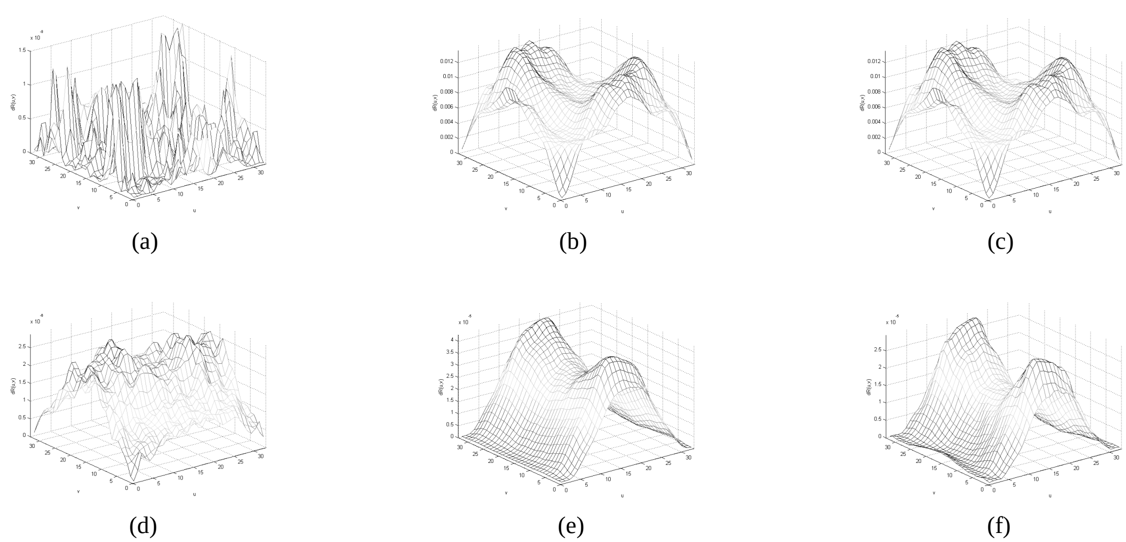

Figure 2: Autocorrelation differences d_R in image patch A between: (a) frame f_1 and frame f_2, (b) frame f_1 and frame f_3, (c) frame f_2 and frame f_3. Autocorrelation differences in image patch B between: (d) frame f_1 and frame f_2, (e) frame f_1 and frame f_3, (f) frame f_2 and frame f_3.

The texture difference d_T between two image patches can be simply calculated by mean square difference of two autocorrelation functions R to compare their similarities,

$$d_T = \frac{1}{(2M+1)(2N+1)} \sum_{u=0}^{2M} \sum_{v=0}^{2N} \left[R_i(u,v) - R_j(u,v) \right]^2, \tag{5}$$

where R_i, R_j are the autocorrelation functions R of two different image patches. The texture differences d_T of image patch A and image patch B between those frames f_1, f_2, f_3 are summarized in Table 1. The texture difference d_T between frame f_1 and frame f_2 for image patch A is extremely small as there is no moving object. The texture difference d_T between frame f_1 and frame f_2 for image patch B is also relatively low even the cast shadow of a bus is projected on the road of frame f_2. Therefore, our observation is satisfied: textural features are only slightly different from those of the corresponding pixels in the background image.

Texture Difference d_T	**Image Patch A**	**Image Patch B**
Frame f_1 and Frame f_2	2.890×10^{-6}	1.724×10^{-3}
Frame f_1 and Frame f_3	9.272	1.923×10^{-2}
Frame f_2 and Frame f_3	9.265	1.071×10^{-2}

Table 1: Texture differences d_T between frames f_1, f_2, f_3 for image patch A and image patch B.

3. METHODOLOGY

3.1 Assumptions

In our extraction methodology, four assumptions are made with respect to the extraction of vehicles. First, the camera is assumed to be stationary and the background is assumed to be stationary too and contains texture primitives, such as the road surface. Second, the light source is assumed to be single and strong, thus illumination difference between the shadow and background is large in intensity. Third, the texture of the road is assumed to be homogenous within the field of view. Illumination changes due to a moving cast shadow are smooth. Forth, same elements have similar texture, and therefore textural features of the different vehicle components are significantly different.

3.2 Method Overview

Under these four assumptions, the moving objects of an input image frame f_i can be reasonably extracted from the background, where the background reference frame f_b is estimated by the running mode and running average algorithms [11]. In the proposed extraction algorithm as depicted in Figure 3, three likelihood maps L_T, L_Y, L_C are initially created according to the differences in texture, luminance and chrominance between the input image frame f_i and background reference frame f_b. A united likelihood map L_U is then constructed by performing a logical OR operation of those likelihood maps L_T, L_Y, L_C. Finally, a foreground mask is constructed by performing morphological operations. This method has an inherent advantage that cast shadow regions are automatically removed as they have the same textural property as the background.

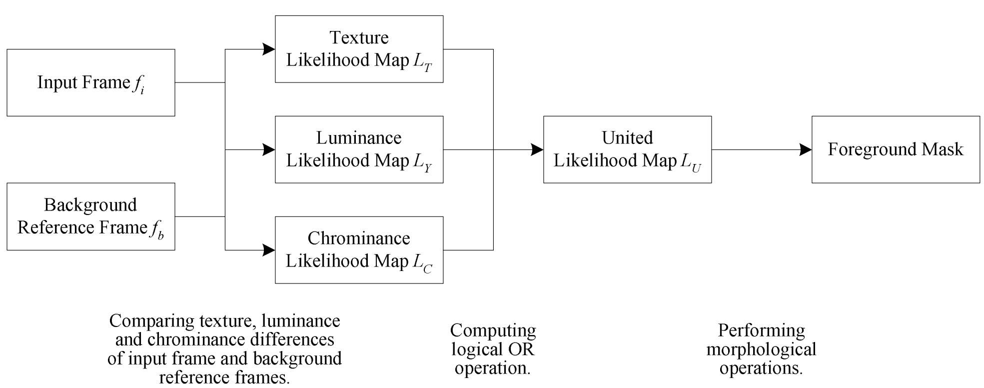

Figure 3: Overview of proposed vehicle extraction method.

After extracting the foreground mask, different components within the mask can be further segmented by simply lowering the number of quantization levels of a foreground object. Many segmentation methods have been proposed [9, 17]. However, their segmented regions cannot be further categorized. With the description of textural feature in each region, different components can be further categorized based on the similarities between segmented regions as depicted in Figure 4.

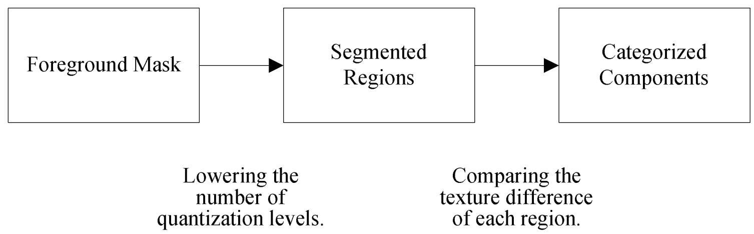

Figure 4: Categorizing vehicle components from an extracted mask.

3.3 Details of the Method

The first task of vehicle extraction is to construct a texture likelihood map L_T. In this step, each pixel with its neighborhood from an input image frame f_i is transformed to be defined an input image patch p_i, and its same neighborhood from a background reference frame f_b are transformed to be defined a background image patch p_b,

$$p_{(x,y)}(m,n) = f\left(x+m-M,\, y+n-N\right) \qquad \begin{matrix} 0 \le m \le 2M \\ 0 \le n \le 2N. \end{matrix} \tag{6}$$

A map of texture difference d_T is then constructed as shown in Figure 5 according to the mean square difference of two autocorrelation functions R of each input image patch p_i with the same location of background image patch p_b,

$$d_T(x,y) = \frac{1}{(2M+1)(2N+1)} \sum_{u=0}^{2M} \sum_{v=0}^{2N} \left[R_{(x,y),i}(u,v) - R_{(x,y),b}(u,v) \right]^2 \qquad \begin{matrix} M \le x \le X-M-1 \\ N \le y \le Y-N-1. \end{matrix} \tag{7}$$

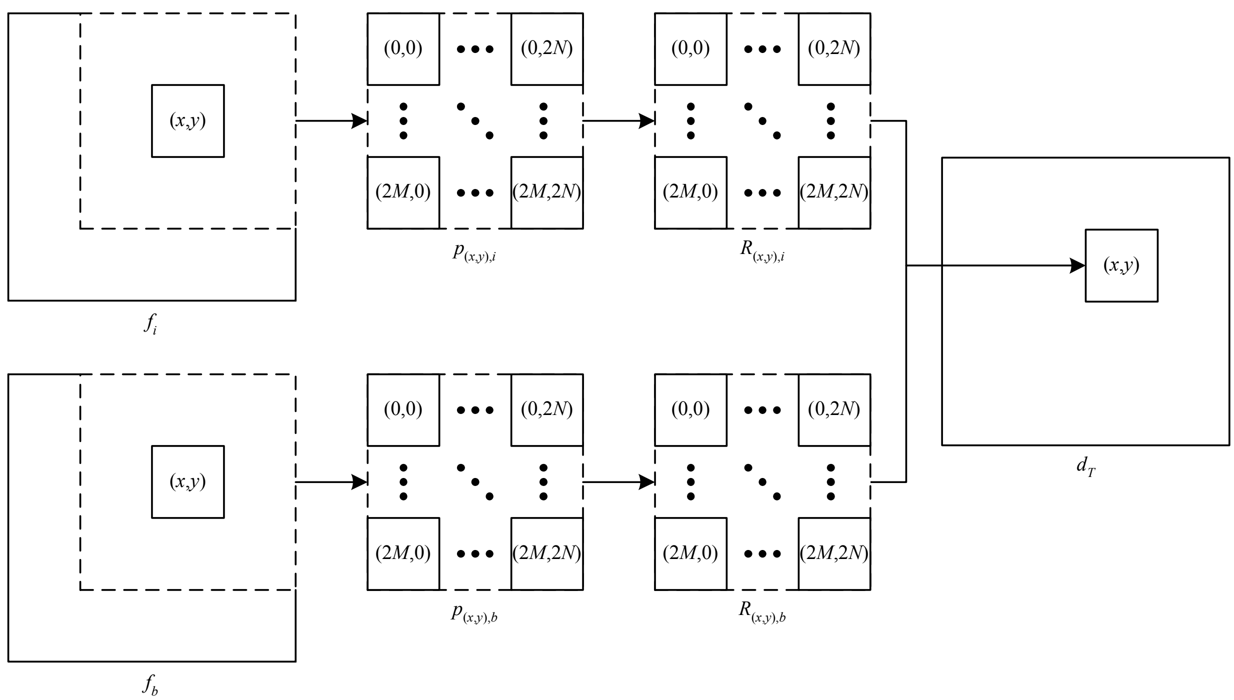

Figure 5: Constructing a texture difference map d_T.

A texture likelihood map L_T is then computed by comparing the texture threshold τ_T with the texture difference map d_T,

$$L_T(x,y) = \begin{cases} 1 & d_T(x,y) > \tau_T \\ 0 & otherwise \end{cases} \qquad \begin{matrix} M \le x \le X - M - 1 \\ N \le y \le Y - N - 1. \end{matrix} \tag{8}$$

The second task of vehicle extraction is to construct a luminance likelihood map L_Y and a chrominance likelihood map L_C. In this step, the color model YCbCr is used to separate the luminance and chrominance components of the images [15]. A luminance difference map d_Y between the input image frame f_i and the background reference frame f_b is constructed according to the following equation,

$$d_Y(x,y) = \begin{cases} Y_i(x,y) - Y_b(x,y) & Y_i(x,y) - Y_b(x,y) > 0 \\ 0 & otherwise \end{cases} \qquad \begin{matrix} M \le x \le X - M - 1 \\ N \le y \le Y - N - 1, \end{matrix} \tag{9}$$

and a chrominance difference map d_C between input image frame f_i and background reference frame f_b is constructed according to the following equation,

$$d_C(x,y) = \left[Cb_i(x,y) - Cb_b(x,y)\right]^2 + \left[Cr_i(x,y) - Cr_b(x,y)\right]^2 \qquad \begin{matrix} M \le x \le X - M - 1 \\ N \le y \le Y - N - 1. \end{matrix} \tag{10}$$

Both the luminance likelihood map L_Y and chrominance likelihood map L_C are then calculated by comparing the luminance threshold τ_L and chrominance threshold τ_C with the luminance difference map d_Y and luminance difference map d_C respectively,

$$L_Y(x,y) = \begin{cases} 1 & d_Y(x,y) > \tau_Y \\ 0 & otherwise \end{cases} \qquad \begin{matrix} M \le x \le X - M - 1 \\ N \le y \le Y - N - 1, \end{matrix} \tag{11}$$

$$L_C(x,y) = \begin{cases} 1 & d_C(x,y) > \tau_C \\ 0 & otherwise \end{cases} \qquad \begin{matrix} M \le x \le X - M - 1 \\ N \le y \le Y - N - 1. \end{matrix} \tag{12}$$

Finally, the united likelihood map L_U is computed by a basic logical OR operation of the texture likelihood map L_T, luminance likelihood map L_Y and chrominance likelihood map L_C,

$$L_U(x,y) = L_T(x,y) + L_Y(x,y) + L_C(x,y) \qquad \begin{matrix} M \le x \le X - M - 1 \\ N \le y \le Y - N - 1. \end{matrix} \tag{13}$$

There are many algorithms for selecting optimal threshold such as isodata algorithm, background-symmetry algorithm and triangle algorithm. However, there is no universal approach for threshold selection that is guaranteed to work for all images. In this paper, the optimal setting of parameters τ_T, τ_Y and τ_C are determined by the isodata algorithm as isodata algorithm is simple, automatic and the error rate is low when compared with human justification [14]. According to equations (7), (9) and (10), the values of texture difference map d_T, luminance difference map d_Y and chrominance difference map d_C are between 0 and 1, where the highest intensity and lowest intensity of an image frame are 0 and 1 respectively. Therefore, the technique for choosing thresholds for texture difference map d_T, luminance difference map d_Y and chrominance difference map d_C are the same.

Isodata algorithm is based on an iterative technique. The values of texture difference map d_T, luminance difference map d_Y and chrominance difference map d_C are firstly quantized into the number of levels 2^B, where B is any positive integer. The histogram of each difference map is then constructed. Figure 6 depicts the histogram of luminance difference map d_Y of motorcycle test case in section 4. Each histogram is segmented into two parts using a starting threshold value such as $\tau_0 = 2^{B-1}$, half of the maximum dynamic range. The sample mean $m_{f,0}$ of the difference values associated with the foreground pixels and the sample mean $m_{b,0}$ of the difference values associated with the background pixels are computed,

$$m_{b,0} = \frac{1}{\sum_{i=0}^{2^{B-1}-1} h[i]} \sum_{i=0}^{2^{B-1}-1} h[i]i, \qquad m_{f,0} = \frac{1}{\sum_{i=2^{B-1}}^{2^B-1} h[i]} \sum_{i=2^{B-1}}^{2^B-1} h[i]i, \tag{14}$$

where $h[i]$ is number of pixels at position i. A new threshold value τ_1 is computed as the average of these two sample means. The process is repeated, based upon the new threshold,

$$\tau_k = \frac{m_{f,k-1} + m_{b,k-1}}{2}, \tag{15}$$

until the threshold value does not change any more, $\tau_k = \tau_{k-1}$.

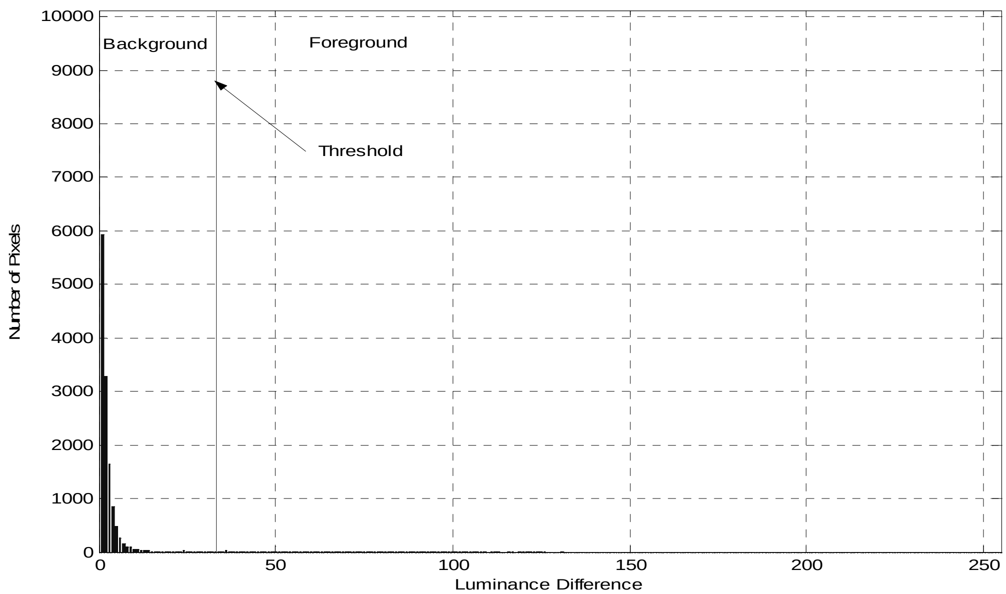

Figure 6: Histogram of luminance difference map d_Y with B = 8 for the motorcycle test case in section 4.

4. SIMULATION RESULTS AND DISCUSSION

Some typical outdoor traffic image sequences on different roads in Hong Kong have been captured in order to test the effectiveness and robustness of the proposed method. The image sequences were captured under different lighting conditions; including sunny, cloudy, and different time of the day with the camera position either overhead or by the roadside. The proposed method was tested under different lighting conditions, viewing angles, vehicle sizes and colors. Some of the images were selected to illustrate the working of the proposed method.

In the first case, an input image frame f_i of a motorcycle is shown in Figure 7(a). In Figure 7(b), a background reference frame f_b was generated by the background estimation algorithm [11]. In Figures 7(c), 7(d), 7(e) and 7(f), the results of texture likelihood map L_T, luminance likelihood map L_Y, chrominance likelihood map L_C and united likelihood map L_U are shown respectively. The vehicle mask can be created by performing the morphological operations: The background noise can be initially detached by performing morphological erosion as shown in Figure 7(g), and then the inner boundaries can be removed by performing morphological dilation on opening as shown in Figure 7(h). Finally the vehicle mask can be restored by performing morphological closing of opening as shown in Figures 7(i). The contour of the vehicle can be created by subtracting the morphological erosion from the vehicle mask as shown in Figure 7(j) and the extracted vehicle can be bounded by the vehicle mask as shown in Figure 7(k). The moving motorcycle can be well extracted with our method while preserving the concavity of the vehicle as the convex hull is not applied to the vehicle mask. Also the region corresponding to the black tires can also be extracted without being classified as the region of cast shadow. However, a narrow background region near to the tires is also extracted as foreground region.

Our method also works well with dark colored vehicle as shown in Figure 8(a) even the luminance values of the vehicle are lower than the cast shadow. The final extracted vehicle is depicted in Figure 8(h). All parts of the dark colored vehicle can be extracted and the cast shadow near to the end of the vehicle was successfully removed. However, the area of the umbra region near to the tires and a small part of background region next to the left side mirror are also extracted as part of the vehicle.

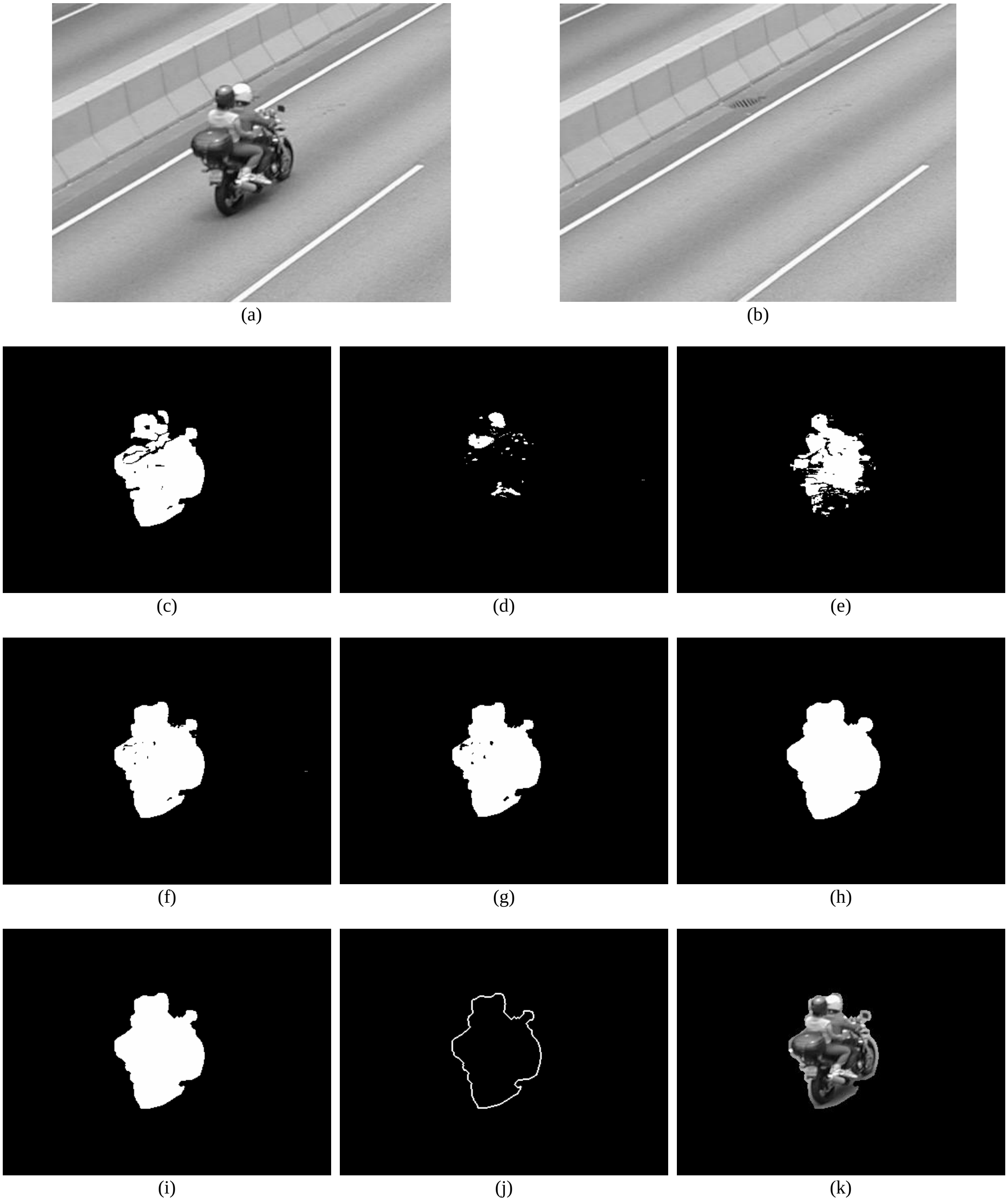

Figure 7: Motorcycle case: (a) Input image frame f_i; (b) Background reference frame f_b; (c) Texture likelihood map L_T; (d) Luminance likelihood map L_Y; (e) Chrominance likelihood map L_C; (f) United likelihood L_U; (g) Morphological erosion; (h) Morphological dilation on opening; (i) Vehicle mask; (j) Contour; (k) Extracted vehicle.

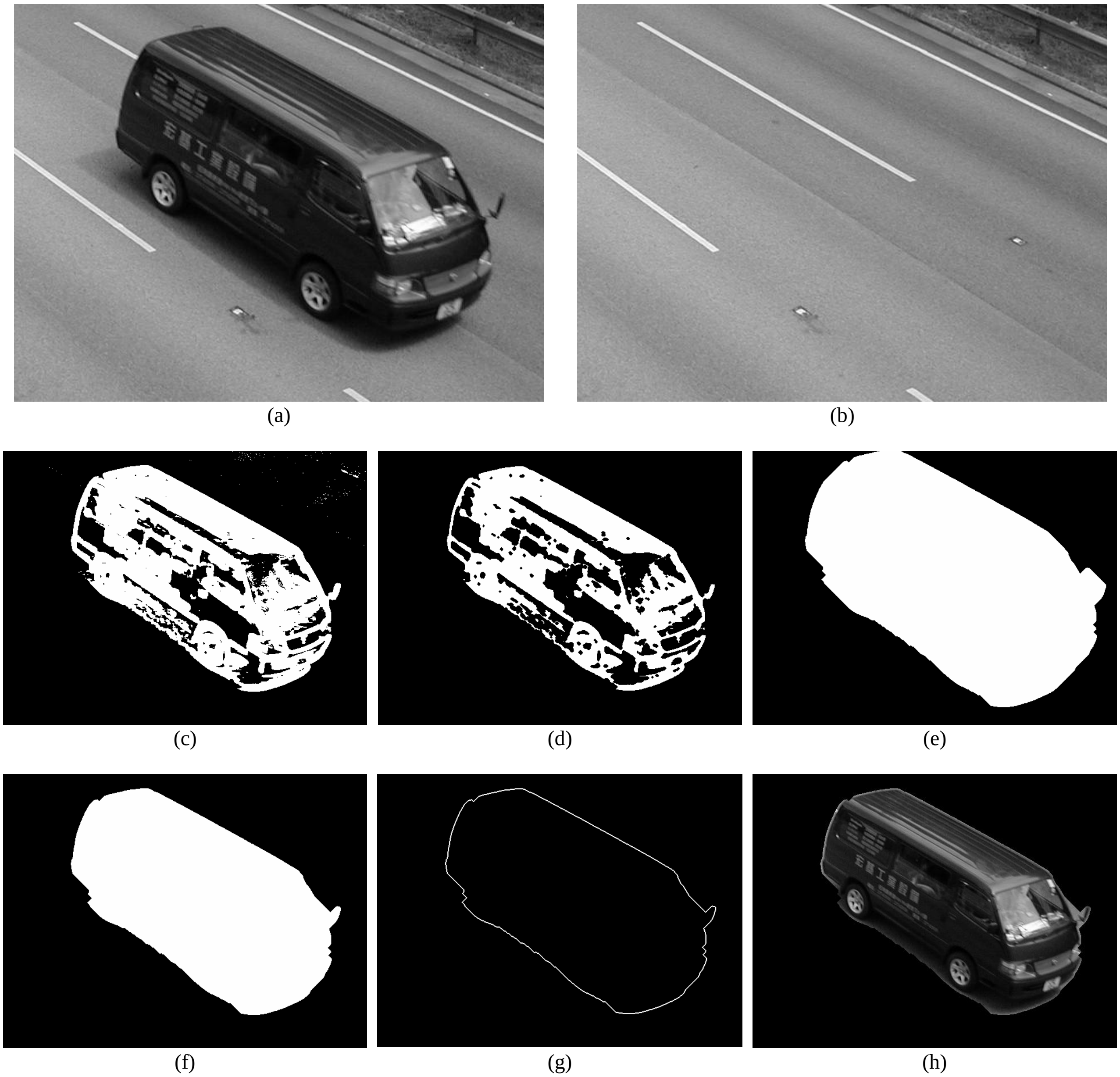

Figure 8: Dark vehicle case: (a) Input image frame f_i; (b) Background reference frame f_b; (c) United Likelihood map L_U; (d) Morphological erosion; (e) Morphological dilation on opening; (f) Vehicle mask; (g) Contour; (h) Extracted vehicle.

In the third case, the results of extracting a taxi under different lighting conditions are shown in Figure 9. The light source was only partially projected on the road as there were some buildings along the road where their cast shadows can be seen in Figure 9(b). The final extracted vehicle is depicted in Figure 9(h). All parts of the taxi are extracted successfully and the cast shadow is automatically removed. However, the area of the umbra region at the back of the taxi is also extracted as foreground region.

In the forth case, the results of extracting a white vehicle under a cloudy weather condition are shown in Figure 10. The final extracted vehicle is shown in Figure 10(f). All parts of the vehicle are extracted, but the umbra regions beside and in front of the white vehicle, and a small part of background region next to the left side mirror are also extracted as foreground region. Further classification of segmented regions of the white vehicle is shown in Figure 11.

Figure 9: Taxi case: (a) Input image frame f_i; (b) Background reference frame f_b; (c) United Likelihood map L_U; (d) Morphological erosion; (e) Morphological dilation on opening; (f) Vehicle mask; (g) Contour; (h) Extracted vehicle.

Figure 11(a) shows different segmented regions by lowering the number of quantization levels. However different regions may belong to the same component of the vehicle. Fore example, Regions A, B and C are segmented into three regions, but regions A and B should be considered as the one region, and therefore the evaluation of three regions are A, B and C calculated by the autocorrelation difference as shown in Figures 11(a), 11(b) and 11(c) respectively. It is obvious that the profiles of autocorrelation function R of region A and region B are similar, but significantly different than the profile of autocorrelation function R of region C.

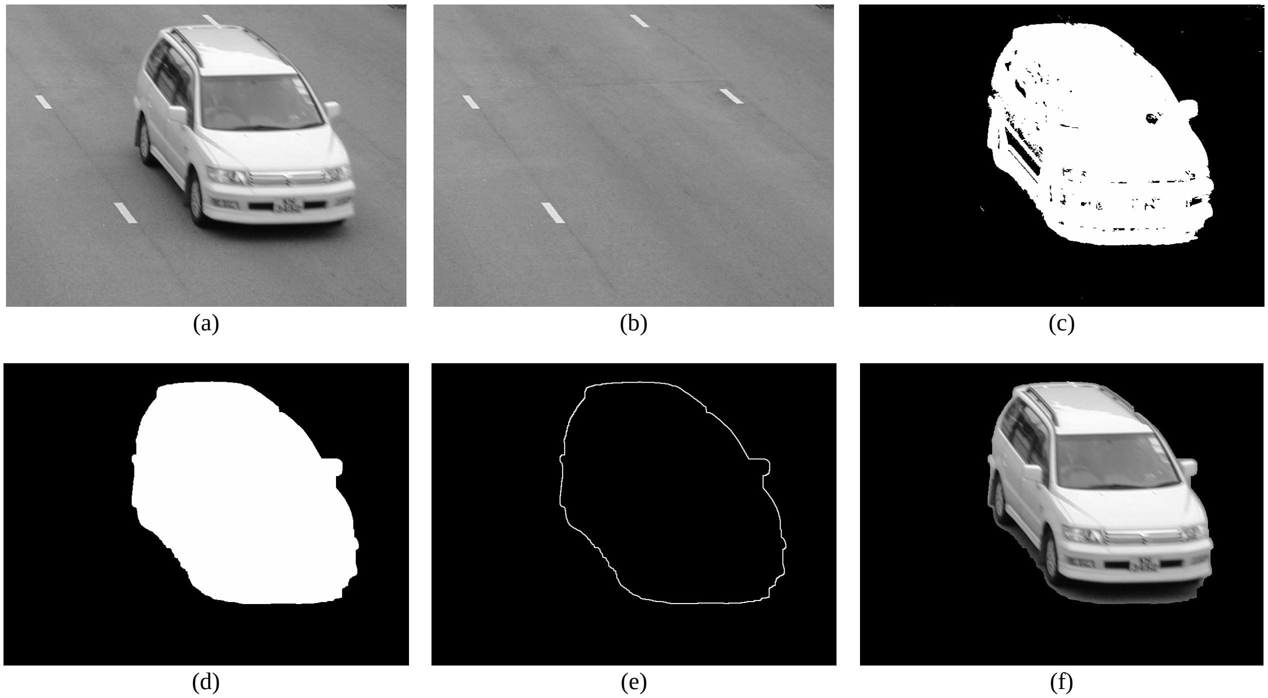

Figure 10: White vehicle case: (a) Input image frame f_i; (b) Background reference frame f_b; (c) United Likelihood map L_U; (d) Vehicle mask; (e) Contour; (f) Extracted vehicle.

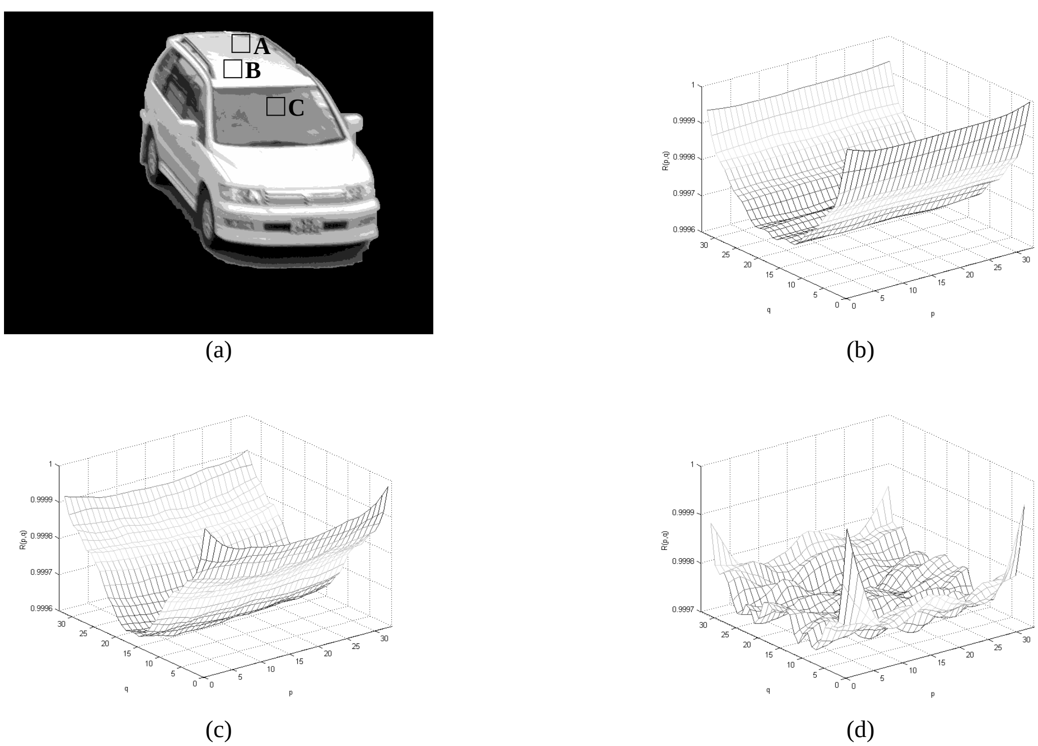

Figure 11: Region classification. (a) Segmented regions of the white vehicle; Profiles of autocorrelation function R of region: (b) A, (c) B, (d) C.

5. CONCLUSIONS

In this paper we have presented an efficient method for extracting moving objects, which can effectively separate the cast shadow from the vehicle under different environment and vehicle color. In this method, a united likelihood map is constructed based on three different domains: texture, luminance and chrominance. A foreground mask can be subsequently computed by performing the morphological operations of the united likelihood map. Also, segmented regions can be categorized into different components according to the autocorrelation index. We have tested our proposed method on different vehicle samples under typical outdoor scenes. Our proposed method is tested to be successful for various outdoor daylight environments and vehicles. Our extensive simulations demonstrated that moving objects can be well extracted while preserving object concavity. It also has an advantage that cast shadow regions are automatically removed as they have the same textural feature as the background reference frame.

6. REFERENCES

1. A. Branca, G. Attolico, A. Distante, "Cast shadow removing in foreground segmentation," *16th International Conference on Pattern Recognition*, vol. 1, pp. 214-217, Aug. 2002.
2. R. Cucchiara, C. Crana, M. Piccardi, A. Prati, S. Sirotti, “Improving shadow suppression in moving object detection with HSV color information,” *IEEE Intelligent Transportation Systems Conference*, pp. 334-339, Aug. 2001.
3. R. Cucchiara, M. Piccardi, P. Mello, "Image analysis and rule-based reasoning for a traffic monitoring system," *IEEE Transactions on Intelligent Transportation Systems*, vol. 1, no. 2, pp. 119-130, Jun. 2000.
4. R. Cucchiara, M. Piccardi, A. Prati, N. Scarabottolo, "Real-time detection of moving vehicles," *International Conference on Image Analysis and Processing*, pp. 618-623, Sept. 1999.
5. N. Doulamis, A. Doulamis, Y. Avrithis, S. Kollias, "A stochastic framework for optimal key frame extraction from MPEG video databases," *IEEE 3rd Workshop on Multimedia Signal Processing*, pp. 141-146, Sept. 1999.
6. A. Elgammal, D. Harwood, L. Davis, “Non-parametric Model for Background Subtraction,” *6th European Conference on Computer Vision*, pp. 751-767, Jun. 2000.
7. G. Fung, N. Yung, G. Pang, A. Lai, “Towards detection of moving cast shadows for visual traffic surveillance,” *EEE Systems, Man, and Cybernetics Conference*, vol. 4, pp. 2505-2510, 2001.
8. R. Haralick, “Statistical and structural approaches to texture,” *Proceedings IEEE*, 67(5):786-804, 1979.
9. C. Kim, J. Hwang, “Fast and automatic video object segmentation and tracking for content-based applications,” *IEEE Transactions on Circuits and Systems for Video Technology*, vol. 12, no. 2, pp. 122-129, Feb. 2002.
10. A. Lai, G. Fung, N. Yung, “Vehicle type classification from visual-based dimension estimation,” *IEEE Intelligent Transportation Systems Conference*, pp. 201-206, Aug. 2001.
11. A. Prati, I. Mikic, C. Grana, M. Trivedi, "Shadow detection algorithms for traffic flow analysis: a comparative study," *Proceedings of IEEE Intelligent Transportation Systems*, pp. 340-345, Aug. 2001.
12. A. Rajagopalan, R. Chellappa, "Vehicle detection and tracking in video," *International Conference on Image Processing*, vol. 1, pp. 351-354, Sept. 2000.
13. A. Rydberg, G. Borgefors, "Integrated method for boundary delineation of agricultural fields in multispectral satellite images," *IEEE Transactions on Geoscience and Remote Sensing*, vol.39, no. 11, pp. 1678-1680, Jul. 2000.
14. E. Salvador, A. Cavallaro, T. Ebrahimi, "Shadow identification and classification using invariant color models," *IEEE International Conference on Acoustics, Speech, and Signal Processing*, vol. 3, pp. 1545-1548, May 2001.
15. J. Stander, R. Mech, J. Ostermann, "Detection of moving cast shadows for object segmentation," *IEEE Transactions on Multimedia*, vol. 1, no. 1, pp.65-76, Mar. 1999.
16. Y. Tsaig, A. Averbuch, "Automatic segmentation of moving objects in video sequences: a region labeling approach," *IEEE Transactions on Circuits and Systems for Video Technology*, vol. 12, no. 7, pp. 597-612, Jul. 2002.
17. M. Yamada, K. Ueda, I. Horiba, N. Sugie, “Discrimination of the road condition toward understanding of vehicle driving environments,” *IEEE Transactions on Intelligent Transportation Systems*, vol. 2, no. 1, pp. 26-31 , Mar, 2001.
18. N. Yung, A. Lai, “A system architecture for visual traffic surveillance,” *5th World Congress on Intelligent Transport Systems*, Oct. 1998.